

Tikhonov Regularization of Circle-Valued Signals

Laurent Condat

April 20, 2022

Abstract—It is common to have to process signals or images whose values are cyclic and can be represented as points on the complex circle, like wrapped phases, angles, orientations, or color hues. We consider a Tikhonov-type regularization model to smoothen or interpolate circle-valued signals defined on arbitrary graphs. We propose a convex relaxation of this nonconvex problem as a semidefinite program, and an efficient algorithm to solve it.

Index Terms—circle-valued data, Tikhonov regularization, smoothing, convex relaxation, directional statistics

I. INTRODUCTION

IN a wide range of applications, one has to deal with signals or images with cyclic, or circular, values, like phases, angles, orientations, or color hues, which are defined modulo π or 2π . Cyclic data appear, for instance, in interferometric synthetic aperture radar [1], color image restoration in HSV or LCh spaces, profilometry [2], Magnetic Resonance Imaging [3], biology, with data on the bacterial flagellar motor [4], in times series of wind directions [5], or in social sciences [6].

A cyclic value can be represented by a point on the complex circle; that is, a complex number of the form $e^{j\omega}$, for some phase $\omega \in \mathbb{R}$, where $j = \sqrt{-1}$. Equivalently, the value is represented by its wrapped phase $\omega \in (-\pi, \pi]$, and the signal presents artificial 2π jumps when the values cross the π or $-\pi$ boundaries. Thus, to denoise or estimate circle-valued data, an option is to *unwrap* the phase map to remove these artificial discontinuities, by estimating the lost integer multiples of 2π in the phase values. Then the unwrapped signal or image can be processed using standard techniques for scalar data. Unfortunately, image unwrapping is a notoriously difficult problem [7]–[9], and the unwrapping process is prone to errors, so that it is preferable to process circle-valued data by keeping them on the circle.

We consider the general setting, where a signal is defined on a graph, with values located at the nodes. Two values are adjacent if there is an edge between their nodes. A 2-D image is a particular case with edges between every pair of neighboring pixels horizontally and vertically, forming a square grid. Then, to regularize signals on graphs, it is natural to promote the property that adjacent values are close to each other, in some sense. For scalar values, Tikhonov regularization consists in penalizing the squared differences of adjacent values and total variation (TV) regularization [10]–[12] consists, instead, in penalizing the absolute values of these

differences. In this work, we focus on Tikhonov regularization for circle-valued signals. A few methods have been proposed for TV regularization of circle-valued signals [13]–[15], but there seems to be no available method for Tikhonov regularization of circle-valued data, with the exception of [14], where an iterative method based on the proximal point algorithm is proposed, which converges to a local minimum for this type of problems on Hadamard manifolds, which the circle is not. Thus, we tackle the difficult nonconvex problem of Tikhonov regularization for circle-valued signals on graphs, by proposing a new convex relaxation.

The paper is organized as follows: in Section II, we discuss different formulations for the regularization of circle-valued signals. In Section III, we propose a convex relaxation of the considered nonconvex problem, and in Section IV, we propose an algorithm to solve it. In Section V, we illustrate the benefits of the proposed approach with several experiments.

II. TIKHONOV SMOOTHING FOR CIRCLE-VALUED SIGNALS

A. Circle-Valued Signals on Graphs

Let $\mathbb{S} = \{z \in \mathbb{C} : |z| = 1\}$ denote the complex unit circle. We want to estimate a signal $x = (x_n)_{n \in V}$, with values $x_n \in \mathbb{S}$, defined on a connected undirected graph (V, E) , where V is the set of nodes and E is the set of edges, which are sets of two distinct nodes. Typically, we are given a noisy signal $y = (y_n)_{n \in V}$ defined on the same graph and the sought signal x is a smoothed, or denoised, version of y , which achieves a tradeoff between closeness to y and smoothness, in some sense. Another typical setting is interpolation, or inpainting: y is defined on a subset $U \subset V$ of nodes and we want to estimate its missing samples; that is, x is the smoothest signal defined on V such that $x_n = y_n$, for every $n \in U$.

B. Classical Tikhonov Regularization

For real-valued signals, Tikhonov-regularized smoothing consists in solving the following convex optimization problem. Given $y = (y_n)_{n \in V}$ and nonnegative weights $(w_n)_{n \in V}$ and $(\lambda_{n,n'})_{\{n,n'\} \in E}$, $x = (x_n)_{n \in V}$ is the solution to

$$\underset{x_n \in \mathbb{R} : n \in V}{\text{minimize}} \quad \sum_{n \in V} \frac{w_n}{2} (x_n - y_n)^2 + \sum_{\{n,n'\} \in E} \frac{\lambda_{n,n'}}{2} (x_n - x_{n'})^2. \quad (1)$$

L. Condat is with King Abdullah University of Science and Technology (KAUST), Thuwal 23955-6900, Kingdom of Saudi Arabia. Contact: see <https://lcondat.github.io/>

For the interpolating task with y defined only on $U \subset V$, we want to solve, instead:

$$\underset{x_n \in \mathbb{R} : n \in V}{\text{minimize}} \sum_{\{n, n'\} \in E} \frac{\lambda_{n, n'}}{2} (x_n - x_{n'})^2 \quad \text{s.t.} \quad x_n = y_n, \forall n \in U. \quad (2)$$

Formally, (2) can be viewed as a particular case of (1) with $w_n = \{+\infty \text{ if } n \in U, 0 \text{ otherwise}\}$, so that we can focus on the form (1), with the weights w_n allowed to be $+\infty$.

We want to formulate an equivalent problem to (1) for signals x and y with values in \mathbb{S} . Let us define the argument function \arg , which maps $z \in \mathbb{S}$ to $\arg(z) \in (-\pi, \pi]$, such that $z = e^{j\arg(z)}$. A natural adaptation to circle-valued signals is to replace the squared Euclidean distance $(t, t') \in \mathbb{R}^2 \mapsto (t - t')^2$ by the geodesic distance $(z, z') \in \mathbb{S}^2 \mapsto \min(|\arg(z) - \arg(z')|, 2\pi - |\arg(z) - \arg(z')|)$. This yields a nonconvex and nonsmooth, therefore very difficult, optimization problem to solve. In this work, we consider instead a statistical view of the estimation problem, which leads to a different formulation.

C. Bayesian View

We can notice that (1) corresponds to the maximum-a-posteriori (MAP) estimate of an unknown signal x^\sharp given y , which is x^\sharp plus white Gaussian noise, assuming a Gaussian Markov Random Field prior for x^\sharp , with nonzero dependencies between its Gaussian variables along the edges of V . That is, $y_n - x_n^\sharp \sim \mathcal{N}(1/w_n)$ and $x_n^\sharp - x_{n'}^\sharp \sim \mathcal{N}(1/\lambda_{n, n'})$, where $\mathcal{N}(\sigma^2)$ denotes the normal distribution with zero mean and variance σ^2 . Thus, in the circle-valued case, let us consider that $y_n = e^{j\alpha_n}$ is a noisy version of $x_n^\sharp = e^{j\omega_n^\sharp}$, in the sense that $\alpha_n \in \mathbb{R}$ is $\omega_n^\sharp = \arg(x_n^\sharp) \in (-\pi, \pi]$ plus Gaussian noise. Then $\arg(y_n)$, which is the wrapped version in $(-\pi, \pi]$ of $\alpha_n \in \mathbb{R}$, follows the wrapped normal distribution with mean ω_n^\sharp . Since its probability density function (p.d.f.) does not have a closed form, it is common in directional statistics to consider instead, as a close approximation, the von Mises distribution [16]. That is, we consider that $\arg(y_n)$ is the outcome of a random variable with p.d.f. $\propto e^{w_n \cos(\cdot - \omega_n^\sharp)}$. Another argument for the von Mises distribution is that it is the maximum entropy distribution with prescribed ‘variance’ $1/w_n$. Hence, we formulate Tikhonov smoothing for circle-valued signals as the MAP estimate of an unknown Markov Random Field with von Mises dependencies, perturbed by von Mises noise. That is, taking the negative logarithm of the p.d.f., $x_n = e^{j\omega_n}$, where the $\omega_n = \arg(x_n)$ are the solutions to

$$\underset{\omega_n \in (-\pi, \pi] : n \in V}{\text{minimize}} \sum_{n \in V} w_n (1 - \cos(\omega_n - \arg(y_n))) + \sum_{\{n, n'\} \in E} \lambda_{n, n'} (1 - \cos(\omega_n - \omega_{n'})). \quad (3)$$

Note that the Taylor series of $1 - \cos(t)$ is $t^2/2 + o(t^2)$, so that for small deviations, the problems (3) and (1) behave similarly.

D. Proposed Model

Now, we can express the problem (3) with respect to the variables $x_n \in \mathbb{S}$, instead of reasoning on their arguments ω_n .

The problem becomes:

$$\underset{x_n \in \mathbb{S} : n \in V}{\text{minimize}} \sum_{n \in V} w_n (1 - \Re(x_n y_n^*)) + \sum_{\{n, n'\} \in E} \lambda_{n, n'} (1 - \Re(x_n x_{n'}^*)), \quad (4)$$

where \Re denotes the real part and $*$ denotes the complex conjugation. Note that this problem is nonconvex for two reasons: the variables x_n are constrained to live in the nonconvex circle \mathbb{S} and the product $\Re(x_n x_{n'}^*)$ is nonconvex. The second issue can be resolved by noticing that $1 - \Re(x_n x_{n'}^*) = \frac{1}{2}|x_n - x_{n'}|^2$. Indeed $|x_n - x_{n'}|^2 = |x_n x_{n'}^* - 1|^2 = (\Re(x_n x_{n'}^*) - 1)^2 + \Im(x_n x_{n'}^*)^2 = 2 - 2\Re(x_n x_{n'}^*)$, where \Im denotes the imaginary part. Therefore, the problem (4) can be rewritten as:

$$\underset{x_n \in \mathbb{S} : n \in V}{\text{minimize}} \sum_{n \in V} \frac{w_n}{2} |x_n - y_n|^2 + \sum_{\{n, n'\} \in E} \frac{\lambda_{n, n'}}{2} |x_n - x_{n'}|^2, \quad (5)$$

which is the natural extension of (1) in the complex plane, and where the objective function to minimize is convex; there remains the nonconvex circle constraint.

Another motivation for our model (4)–(5) is the following: suppose that y is a corrupted version of the unknown circle-valued signal x^\sharp with complex Gaussian noise; that is, independent Gaussian noise with variance $1/w_n$ is added to the real and imaginary parts of each $x_n^\sharp \in \mathbb{S}$. Then, almost surely, the y_n are no longer in \mathbb{S} . In that case, the MAP estimate of x^\sharp is exactly the solution to (5), where the y_n are now any complex numbers. Moreover, $\frac{1}{2}|x_n - y_n|^2 = \frac{1}{2}(1 + |y_n|^2) - \Re(x_n y_n^*)$, so that the problem (5) can be rewritten as:

$$\underset{x_n \in \mathbb{S} : n \in V}{\text{minimize}} \Psi_{\text{orig}}(x) = \sum_{n \in V} w_n \left(\frac{1}{2}(1 + |y_n|^2) - \Re(x_n y_n^*) \right) + \sum_{\{n, n'\} \in E} \lambda_{n, n'} (1 - \Re(x_n x_{n'}^*)). \quad (6)$$

The problem (6) generalizes (4) to any complex numbers y_n , but since a constant value in the cost function to minimize does not change the solution, (4) and (6) are equivalent.

A natural idea to make the problem (5) convex is to remove the nonconvex circle constraint; we discuss this approach in Section II-F. Instead, we propose to stick with the formulation (6) and we propose a new convex relaxation of this problem, in Section III.

E. Limit Cases

Let us look at the two limit cases of (6), where the data-fit term overwhelms the regularization term, or the other way around. So, let us assume that all w_n are positive and that all $\lambda_{n, n'}$ tend to zero. In that case, the solution is simply $x_n = \{y_n/|y_n| \text{ if } y_n \neq 0, \text{ any point in } \mathbb{S} \text{ otherwise}\}$, for every $n \in V$. The other limit case is more interesting: let us assume that all $\lambda_{n, n'}$ tend to $+\infty$. In that case, the regularization term is minimized, which means that the signal is constant: there exists $x \in \mathbb{S}$ such that $x_n = x$, for every $n \in V$. This point x minimizes the data-fit term $\sum_{n \in V} w_n \Re(x y_n^*) = -\Re(x \sum_{n \in V} w_n y_n^*) = -\Re(x x_{\text{av}}^*)$, where $x_{\text{av}} = \sum_{n \in V} w_n y_n^*$. The solution, called the (weighted) circular mean of the points, is $x = \{x_{\text{av}}/|x_{\text{av}}| \text{ if } x_{\text{av}} \neq 0, \text{ any point in } \mathbb{S} \text{ otherwise}\}$. That

is, \bar{x} is simply the weighted average of the y_n , rescaled to be in \mathbb{S} . Thus, when $w_n \equiv 1$, we have just recovered the well known property that the circular mean of a set of points on the circle is the maximum likelihood estimate of the mean for a von Mises distribution fitting the points.

F. Related Work

There is a large literature about optimization on manifolds. For instance, Bergmann and Tenbrinck [17] proposed a generic approach for smoothing manifold-valued signals on graphs. Weinmann et al. [14] proposed a method for a large class of functionals including the TV and Tikhonov costs, later extended to the Mumford–Shah functional for piecewise smooth reconstruction [18] and to the more general setting of inverse problems [19]. The Potts model can be used for the recovery of piecewise-constant signals [18]. In general, such approaches are heuristic and have no convergence guarantees; when an algorithm is proved to converge, this is typically to a local solution. Here, our goal is to obtain a global and exact minimizer of the nonconvex problem (6), not only a local or approximate minimizer.

Besides variational regularization, methods based on local averaging can be used. For instance, median filtering for circle-valued data has been proposed [20], which is robust to outliers. In the rest of this section, we focus on the *structure tensor* [21]–[25] a popular tool in image processing to analyze and process the local orientation of a vector field, typically the gradient field of an image. Identifying 2-D vectors with complex numbers, let us first recall that $z \in \mathbb{C}$ and $-z$ have same orientation. Defining the orientation as the angle $\omega = \arg(z)$, we can either restrict ω to the interval $[0, \pi)$, or define it on the real line modulo π ; that is $\omega \in \mathbb{R}$ is the same orientation as $\omega + \pi$. Therefore, when processing orientations, to avoid cancellation effects that might happen when averaging numbers similar to z with numbers similar to $-z$, it is better to multiply ω by two, so that it is in $(-\pi, \pi]$, like a phase or angle; that is, one deals with $e^{j2\omega} = z^2$ instead of z . Thus, Tikhonov smoothing for orientations consists in solving (4) with the $y_n \in \mathbb{S}$ replaced by y_n^2 ; then the smoothed values are the $\sqrt{\bar{x}_n}$, to reverse the doubling operation.

Keeping this squaring effect for orientations in mind, the structure tensor method, to smooth a 2-D vector field identified with a complex-valued image y , works as follows: each value $y_n \in \mathbb{C}$ is mapped to the 2×2 real matrix of rank 1

$$M_n = \begin{bmatrix} \Re(y_n)^2 & \Re(y_n)\Im(y_n) \\ \Re(y_n)\Im(y_n) & \Im(y_n)^2 \end{bmatrix}. \quad (7)$$

Note that y_n and $-y_n$ are mapped to the same matrix, which is consistent with the discussion above: in this context, only the vector orientations matter, not their directions. Then the matrices M_n are spatially averaged by applying a lowpass filter to them, elementwise. After filtering, the smoothed matrix \bar{M}_n does not have rank 1, in general. Thus, the smoothed value x_n is obtained by setting $[\Re(x_n) \ \Im(x_n)]^T$ as the principal

eigenvector of \bar{M}_n . To understand this process, let us define $\alpha_n = \arg(y_n)$. We have, for every $n \in V$,

$$\begin{aligned} M_n &= |y_n|^2 \begin{bmatrix} \cos(\alpha_n)^2 & \cos(\alpha_n)\sin(\alpha_n) \\ \cos(\alpha_n)\sin(\alpha_n) & \sin(\alpha_n)^2 \end{bmatrix} \\ &= \frac{|y_n|^2}{2} \begin{bmatrix} 1 & 0 \\ 0 & 1 \end{bmatrix} + \frac{|y_n|^2}{2} \begin{bmatrix} \cos(2\alpha_n) & \sin(2\alpha_n) \\ \sin(2\alpha_n) & -\cos(2\alpha_n) \end{bmatrix}. \end{aligned} \quad (8)$$

After filtering, \bar{M}_n is symmetric and can be written as

$$\begin{aligned} \bar{M}_n &= \begin{bmatrix} m_{n,1} & m_{n,3} \\ m_{n,3} & m_{n,2} \end{bmatrix} \\ &= d_n \begin{bmatrix} 1 & 0 \\ 0 & 1 \end{bmatrix} + a_n \begin{bmatrix} \cos(2\omega_n) & \sin(2\omega_n) \\ \sin(2\omega_n) & -\cos(2\omega_n) \end{bmatrix} \\ &= \begin{bmatrix} 2a_n \cos(\omega_n)^2 + d_n - a_n & 2a_n \cos(\omega_n) \sin(\omega_n) \\ 2a_n \cos(\omega_n) \sin(\omega_n) & 2a_n \sin(\omega_n)^2 + d_n - a_n \end{bmatrix} \\ &= \begin{bmatrix} \cos(\omega_n) & \sin(\omega_n) \\ \sin(\omega_n) & -\cos(\omega_n) \end{bmatrix} \begin{bmatrix} d_n + a_n & 0 \\ 0 & d_n - a_n \end{bmatrix} \\ &\quad \times \begin{bmatrix} \cos(\omega_n) & \sin(\omega_n) \\ \sin(\omega_n) & -\cos(\omega_n) \end{bmatrix}, \end{aligned} \quad (9)$$

with $d_n = (m_{n,1} + m_{n,2})/2$, $a_n = ((m_{n,1} - m_{n,2})^2/4 + m_{n,3}^2)^{1/2} = |x_n|/2$, and $\omega_n = \arg(x_n)/2$, where we set

$$x_n = (m_{n,1} - m_{n,2}) + 2jm_{n,3} = 2a_n e^{j2\omega_n}. \quad (10)$$

Thus, the two eigenvalues of \bar{M}_n , in decreasing order, are $d_n + a_n$ and $d_n - a_n$ and its principal eigenvector is $[\cos(\omega_n) \ \sin(\omega_n)]^T$. a_n is a confidence indicator: if $a_n = 0$, there is no preferred direction locally, whereas if it is large, the direction ω_n is dominant. Thus, we do not need the matrix formalism: reasoning on the complex numbers y_n and x_n is equivalent and easier. Indeed, since $y_n^2 = |y_n|^2 e^{j2\alpha_n} = (\Re(y_n)^2 - \Im(y_n)^2) + 2j\Re(y_n)\Im(y_n)$, x_n is simply the result of spatial averaging applied to the y_n^2 .

Tikhonov regularization amounts to lowpass filtering: with $w_n \equiv 1$ and $\lambda_{n,n'} \equiv \lambda$, the solution x to (5) without the circle constraint is simply the result of a convolution applied to y , with inverse frequency response one plus λ times the graph Laplacian. Therefore, the structure tensor method is essentially solving the Tikhonov problem (5), with the variables searched in \mathbb{C} instead of \mathbb{S} and with the y_n replaced by y_n^2 , this second change being specific to the setting of orientations. Note that if $|y_n| = 1$ for all n , squaring the y_n in (5), with the circle constraint, still corresponds to a MAP estimate with a scaled von Mises prior. However, if the amplitudes $|y_n|$ are arbitrary, squaring the y_n also squares their amplitudes, so that the squared amplitudes are averaged by the regularization process; there seems to be no obvious Bayesian interpretation of (5), with or without the circle constraint, in that case. Thus, it is better to divide M_n by $|y_n|$ in (7) before spatial averaging, which is the way the structure tensor is defined by Knutsson [24].

Finally, let us remark that if $|y_n| = 1$, when solving (5) without the circle constraint, the x_n remain in the convex hull of the y_n , which is contained in the complex disk $\mathbb{D} = \{z \in \mathbb{C} : |z| \leq 1\}$, the convex hull of \mathbb{S} . Thus, there is no need to enforce the constraint that the x_n belong to \mathbb{D} , since it is automatically satisfied. In the sequel, we will refer to the

following process, to find an approximate solution of (5), as the *baseline method*: (5) is solved without the circle constraint (which amounts to solving a linear system) and the x_n are rescaled as $x_n/|x_n|$ afterwards, to make them lie in \mathbb{S} .

III. FOURIER LIFTING: CONVEX RELAXATION USING MOMENTS OF MEASURES

The method of moments – There is a general recipe to reformulate, or *lift*, a nonconvex problem as a convex one: the minimization of a function f over \mathbb{S} is equivalent to minimizing $\int_{\mathbb{S}} f(z) d\mu(z)$ over μ in the set of probability measures (i.e. positive Borel measure with mass 1) on \mathbb{S} , assuming that $\arg \min(f)$, the set of minimizers of f , is nonempty. This latter problem is convex, since it consists in minimizing a linear functional over a convex set. A minimizing measure μ^* will be concentrated over $\arg \min(f)$; in particular, if the minimizer z^* of f is unique, $\mu^* = \delta_{z^*}$, the Dirac measure at z^* . This principled approach has a major downside, yet: the set of probability measures is infinite-dimensional, which prevents its numerical implementation in general. However, there is a case where the method can be implemented exactly: if the measure can be parameterized and recovered from a finite number M of its moments $\hat{\mu}_m = \int_{\mathbb{S}} \phi_m(z) d\mu(z)$, $m = 1, \dots, M$, for some basis functions ϕ_m , and if $f = \sum_{m=1}^M a_m \phi_m$ is a linear combination of the ϕ_m , then $\int_{\mathbb{S}} f(z) d\mu(z) = \sum_{m=1}^M a_m \hat{\mu}_m$, so that the problem becomes convex and finite-dimensional, in terms of the moments $\hat{\mu}_m$: we want to minimize the linear term $\sum_{m=1}^M a_m c_m$ with respect to the coefficients c_m , under the constraint that $c_m = \hat{\mu}_m$ for every m , for some probability measure μ . This approach is called *the method of moments* [26]. In this work, we use trigonometric moments, or Fourier coefficients. The characterization of a measure on the circle from a subset of its Fourier coefficients has a long history, rooted in Carathéodory's work [27]; related theorems are often called Bochner's theorems. In short, the constraint that the $c_m = \hat{\mu}_m$ for some positive measure μ on the circle is satisfied if the Toeplitz matrix formed by the c_m is positive semidefinite [28], [29].

Convex relaxation of optimization over graphs using measures – Our problem (6) features nonconvex pairwise costs $(x_n, x_{n'}) \mapsto \Re(x_n x_{n'}^*)$. The minimization of a function $g(z, z')$ is equivalent to minimizing $\int_{\mathbb{S}^2} g(z, z') d\nu(z, z')$ over ν in the set of probability measures on \mathbb{S}^2 . Hence, given an optimization problem over the graph (V, E) with unary potential costs f_n at the nodes and symmetric pairwise interaction costs $g_{n,n'}$ at the edges, all bounded from below and lower semicontinuous:

$$\underset{x_n \in \mathbb{S} : n \in V}{\text{minimize}} \sum_{n \in V} f_n(x_n) + \sum_{\{n, n'\} \in E} g_{n,n'}(x_n, x_{n'}), \quad (11)$$

we propose the following lifting technique: we introduce a probability measure μ_n on \mathbb{S} for each node $n \in V$, as well as

a probability measure $\nu_{n,n'}$ on \mathbb{S}^2 for each edge $\{n, n'\} \in E$, and we consider the lifted convex problem:

$$\begin{aligned} & \underset{(\mu_n), (\nu_{n,n'})}{\text{minimize}} \sum_{n \in V} \int_{\mathbb{S}} f_n(z) d\mu_n(z) \\ & + \sum_{\{n, n'\} \in E} \int_{\mathbb{S}^2} g_{n,n'}(z, z') d\nu_{n,n'}(z, z') \end{aligned} \quad (12)$$

s.t. the two marginals of $\nu_{n,n'}$ are μ_n and $\mu_{n'}$.

It is important to note that, in general, this convex relaxation is not tight: even if the solution $(x_n^*)_{n \in V}$ to (11) is unique, it is not guaranteed that the solution to (12) corresponds to $\mu_n^* = \delta_{x_n^*}$: it might be that measures which are not Diracs achieve a lower value of the objective function.

Interestingly, there is a strong connection with the theory of optimal transport [30]: the function

$$(\mu_n, \mu_{n'}) \mapsto \min_{\nu_{n,n'}} \int_{\mathbb{S}^2} g_{n,n'}(z, z') d\nu_{n,n'}(z, z') \quad (13)$$

s.t. the two marginals of $\nu_{n,n'}$ are μ_n and $\mu_{n'}$,

is the Monge–Kantorovich optimal transport cost between the probability measures μ_n and $\mu_{n'}$, interpreting $g_{n,n'}(z, z')$ as the cost of moving one unit of mass from the point z to the point z' ; the minimizing measure $\nu_{n,n'}^*$ in (13), which exists, is called the optimal coupling measure. We refer to [31] for more details on optimal transport on the circle \mathbb{S} .

When the measures are restricted to live on a finite set of labels, instead of a continuous set like \mathbb{S} , the relaxation (12), which is a linear program, is well known in statistics, in the fields of graphical models, discrete inference and labeling, where it is called the local polytope relaxation [32]–[34]. In the present work, we do not want to discretize the circle \mathbb{S} . We will instead parameterize the measures by a finite number of their Fourier coefficients, like in the method of moments; hence, we name our convex relaxation approach as *Fourier lifting*.

Fourier lifting – A probability measure ν defined on \mathbb{S}^2 has Fourier coefficients $\hat{\nu}_{m,m'} = \int_{\mathbb{S}^2} z^{-m} z'^{-m'} d\nu(z, z')$ for every $(m, m') \in \mathbb{Z}^2$. We have $\hat{\nu}_{-m, -m'} = \hat{\nu}_{m, m'}^*$ and $\hat{\nu}_{0,0} = 1$.

ν has two marginals $\mu = \int_{\mathbb{S}} d\nu(\cdot, z)$ and $\mu' = \int_{\mathbb{S}} d\nu(z, \cdot)$, which are probability measures on \mathbb{S} . They have Fourier coefficients $\hat{\mu}_m = \int_{(-\pi, \pi]} e^{-jm\omega} \mu(e^{j\omega}) d\omega = \hat{\nu}_{m,0}$ and $\hat{\mu}'_{m'} = \int_{(-\pi, \pi]} e^{-jm'\omega} \mu'(e^{j\omega}) d\omega = \hat{\nu}_{0,m'}$ respectively, for every $(m, m') \in \mathbb{Z}^2$.

If ν is a 2-D Dirac in $(e^{j\omega_1}, e^{j\omega_2}) \in \mathbb{S}^2$, $c_{m,m'} = e^{-j(m\omega_1 + m'\omega_2)} = c_{m,0} c_{0,m'}$, so that the matrix of moments has rank 1 and $|c_{m,m'}| = 1$ for every (m, m') .

In this work, we will only parameterize ν using $c_{0,0} = 1$, $c_{1,0}$, $c_{0,1}$, $c_{-1,1}$. Indeed, if ν is a Dirac in $(e^{j\omega_1}, e^{j\omega_2})$, $c_{1,0} = e^{-j\omega_1}$, $c_{0,1} = e^{-j\omega_2}$, and

$$\cos(\omega_1 - \omega_2) = \int \cos(\omega - \omega') \nu(e^{j\omega}, e^{j\omega'}) d(\omega, \omega') \quad (14)$$

$$= \frac{1}{2}(c_{-1,1} + c_{1,-1}) = \Re(c_{-1,1}). \quad (15)$$

Let us map these coefficients in the 3×3 Hermitian matrix

$$P = \begin{bmatrix} 1 & c_{1,0} & c_{0,1} \\ c_{1,0}^* & 1 & c_{-1,1} \\ c_{0,1}^* & c_{-1,1}^* & 1 \end{bmatrix} \quad (16)$$

P is positive semidefinite, which we denote by $P \succcurlyeq 0$, if and only if all its principal minors are nonnegative; that is,

$$\begin{vmatrix} 1 & c_{1,0} & c_{0,1} \\ c_{1,0}^* & 1 & c_{-1,1} \\ c_{0,1}^* & c_{-1,1}^* & 1 \end{vmatrix} \geq 0, \begin{vmatrix} 1 & c_{1,0} \\ c_{1,0}^* & 1 \end{vmatrix} \geq 0, \quad (17)$$

$$\begin{vmatrix} 1 & c_{0,1} \\ c_{0,1}^* & 1 \end{vmatrix} \geq 0, \begin{vmatrix} 1 & c_{-1,1} \\ c_{-1,1}^* & 1 \end{vmatrix} \geq 0. \quad (18)$$

Equivalently, $|c_{1,0}| \leq 1$, $|c_{0,1}| \leq 1$, $|c_{-1,1}| \leq 1$, $1 + 2\Re(c_{1,0}c_{-1,1}c_{0,1}^*) - |c_{1,0}|^2 - |c_{0,1}|^2 - |c_{-1,1}|^2 \geq 0$.

If ν is a Dirac, $P \succcurlyeq 0$. Thus, for every probability measure ν , by convexity of the positive semidefinite cone, $P \succcurlyeq 0$. Moreover, $P \succcurlyeq 0$ has rank 1 if and only if ν is a Dirac; that is,

$$P = \begin{bmatrix} 1 \\ c_{1,0}^* \\ c_{0,1}^* \end{bmatrix} \begin{bmatrix} 1 & c_{1,0} & c_{0,1} \end{bmatrix}, \quad (19)$$

with $|c_{1,0}| = 1$, $|c_{0,1}| = 1$.

Hence, the proposed convex relaxation of (6) is:

$$\begin{aligned} & \underset{\substack{x_n \in \mathbb{C} : n \in V \\ r_{n,n'} \in \mathbb{C} : (n,n') \in E}}{\text{minimize}} \quad \Psi_{\text{conv}}(x, r) = \sum_{n \in V} w_n \left(\frac{1}{2} (1 + |y_n|^2) - \Re(x_n y_n^*) \right) \\ & \quad + \sum_{\{n,n'\} \in E} \lambda_{n,n'} (1 - \Re(r_{n,n'})) \\ & \text{s.t.} \quad \begin{bmatrix} 1 & x_n^* & x_{n'}^* \\ x_n & 1 & r_{n,n'} \\ x_{n'} & r_{n,n'}^* & 1 \end{bmatrix} \succcurlyeq 0, \quad \forall (n, n') \in E. \end{aligned} \quad (20)$$

A Hermitian positive semidefinite matrix with ones on its diagonal is a correlation matrix, the set of which is sometimes called an elliptope [35]. An elliptope is convex and compact. It is known that a linear function attains its minimum over a compact convex set at a point of its boundary. Since the rank-1 matrices associated to Diracs are extreme points of the elliptope, linear minimization over an elliptope is likely to yield a rank-1 matrix. The convex optimization problem (20) can be viewed as linear minimization over a product of elliptopes with linear equality constraints; there is no guarantee that all matrices in (20) will be of rank 1 at a solution, but this is what we hope for.

Let us call $(x_n^*)_{n \in V}$ and $(r_{n,n'}^*)_{(n,n') \in E}$ a solution obtained by solving (20) and Ψ_{conv}^* the corresponding minimal objective value. We also denote by Ψ_{orig}^* the minimal objective value of the original nonconvex problem (6). If all matrices appearing in (20) are of rank 1, or equivalently $|x_n^*| = 1$ for every $n \in V$ and $r_{n,n'}^* = x_n^* x_{n'}^{**}$ for every $(n, n') \in E$, $\Psi_{\text{conv}}^* = \Psi_{\text{orig}}^*$ and we have obtained an exact solution of the original problem (6). Otherwise, we rescale the x_n^* as $x_n^* / |x_n^*|$ to project them on \mathbb{S} , and we now have an approximate solution x to (6). Let us denote by $\Psi_{\text{approx}} = \Psi_{\text{orig}}(x)$ the objective value evaluated at this x . We have $\Psi_{\text{conv}}^* \leq \Psi_{\text{orig}}^* \leq \Psi_{\text{approx}}$, so that we

can use $(\Psi_{\text{approx}} - \Psi_{\text{conv}}^*) / \Psi_{\text{conv}}^*$ as a measure of relative suboptimality of the convex relaxation with respect to the original problem. We conjecture that the proposed relaxation is tight and yields the exact solution whenever the graph (V, E) has no cycle, as is the case for a 1-D chain.

IV. PROPOSED ALGORITHM

We endow \mathbb{C} with the inner product $\langle z, z' \rangle = \Re(z z'^*)$, to form a real Hilbert space. Then the problem (20) has the form

$$\underset{s \in \mathbb{C}^d}{\text{minimize}} \quad \Psi_{\text{conv}}(s) = \langle s, e \rangle + f(Ls), \quad (21)$$

where the variable s is the concatenation of all x_n and $r_{n,n'}$, the dimension d is the total number of nodes and edges, $e \in \mathbb{C}^d$ is the concatenation of all constants $-w_n y_n$ and $-\lambda_{n,n'}$, the linear operator L maps e to the concatenation of matrices

$$(Le)_{n,n'} = \begin{bmatrix} 0 & x_n^* & x_{n'}^* \\ x_n & 0 & r_{n,n'} \\ x_{n'} & r_{n,n'}^* & 0 \end{bmatrix} \quad (22)$$

for all $(n, n') \in E$, $f : (Q_{n,n'})_{(n,n') \in E} \mapsto \sum_{(n,n') \in E} \{0 \text{ if } Q_{n,n'} + \text{Id} \succcurlyeq 0, +\infty \text{ otherwise}\}$, and Id is the 3×3 identity matrix. We endow the set of 3×3 Hermitian matrices with the Frobenius inner product $\langle Q, Q' \rangle = \text{tr}(Q Q')$, where tr denotes the trace.

To solve the problem (21), a well suited algorithm is the Proximal Method of Multipliers [36], [37], which, initialized with some variables $U^{(0)} \in (\mathbb{C}^{3 \times 3})^{|E|}$ and $s^{(0)} \in \mathbb{C}^d$, consists in the iteration: for $i = 0, 1, \dots$

$$\begin{cases} a^{(i)} = L^* U^{(i)} + e \\ s^{(i+1)} = s^{(i)} - \tau a^{(i)} \\ U^{(i+1)} = \text{prox}_{\sigma f^*}(U^{(i)} + \sigma L(s^{(i+1)} - \tau a^{(i)})) \end{cases}$$

where L^* denotes the adjoint operator of L , f^* denotes the convex conjugate of f [38], $\tau > 0$ is a parameter, and we set $\sigma = 1/(\|L\|^2 \tau)$, where the squared operator norm $\|L\|^2$ is twice the maximum number of edges per node. With this choice, the variable $s^{(i)}$ in the algorithm converges to a solution s^* of (21) [37, Theorem 4.3]. In the algorithm, the proximity operator $\text{prox}_{\sigma f^*}$ maps each matrix $Q_{n,n'}$, for $(n, n') \in E$, to the projection of $Q_{n,n'} + \sigma \text{Id}$ onto the cone of Hermitian negative semidefinite matrices, minus σId ; this is achieved by computing the eigendecomposition and setting the positive eigenvalues to zero.

V. EXPERIMENTS

For the following experiments, MATLAB code implementing the algorithms and generating the images in the figures is available on the author's webpage. The code was run in MATLAB R2022a on a Apple Macbook Pro 2019 laptop.

A. Denoising of a 1-D signal

In a first experiment, we denoise a 1-D signal of size $N = 1000$. That is, $V = \{1, \dots, N\}$ and $E = \{(1, 2), \dots, (N-1, N)\}$. The ground-truth signal $(e^{j\omega_n^\#})_{n \in V}$ is generated using $\omega_1^\# = 1$ and i.i.d random increments $\omega_{n+1}^\# - \omega_n^\#$ following the Gaussian law of standard deviation 0.1. Then the noisy signal

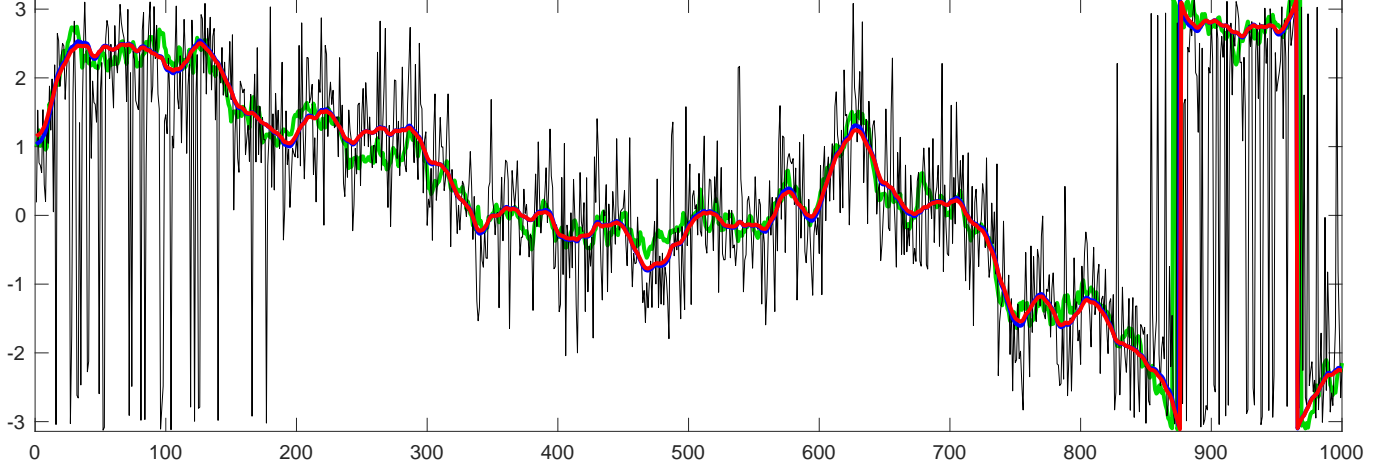


Fig. 1. Denoising of a circle-valued signal. In green, the ground-truth signal, in black, the noisy signal, in blue, the signal denoised with the baseline method and in red, the signal $(x_n^*)_{n \in V}$ denoised with the proposed approach, which turns out to be the exact solution to (4). All signals have their values in \mathbb{S} , whose argument in $(-\pi, \pi]$ is displayed.

y is formed by adding to the $\omega_n^\#$ white Gaussian noise of standard deviation $\sqrt{\lambda}/10$, where $\lambda = 50$. These two signals are shown in Fig. 1 in green and black, respectively. We denoise y using the baseline method described at the end of Section II, with $\omega_n \equiv 1$ and $\lambda_{n,n'} \equiv \lambda$; the denoised signal is shown in blue in Fig. 1. The corresponding cost value in (6), or equivalently in (3), (4), or (5), is $\Psi_{\text{orig}}(x) \approx 227$. Then we apply the proposed approach by solving (20), with $\tau = 0.1$ in the algorithm, which converges to machine precision in about 300 iterations. The obtained denoised signal, shown in red in Fig. 1, satisfies $|x_n^*| = 1$ and $r_{n,n+1}^* = x_n^* x_{n+1}^{**}$ for every n , so that it is the exact solution to the original problem (6). The corresponding optimal cost value is $\Psi_{\text{conv}}^* = \Psi_{\text{orig}}^* \approx 226$. The quantitative and qualitative difference between the results of the baseline and proposed methods is small in this example, but it is satisfying to be able to solve the nonconvex problem of Tikhonov smoothing exactly.

B. Denoising of a 2-D image

In a second experiment, we denoise a 2-D image: the phase of a smooth ground-truth image of size 97×97 is generated by cubic interpolation from a random 4×4 image and white Gaussian noise of standard deviation 0.5 is added to the phases to obtain a noisy version y ; they are shown in Fig. 2 (a) and (b), respectively. The graph is the classical square grid: there is a node at each pixel and the edges connect all pairs of horizontally or vertically adjacent pixels. We denoise y using the baseline method described at the end of Section II, with $\omega_n \equiv 1$ and $\lambda_{n,n'} \equiv \lambda = 5$ (with 400 iterations, computation time 0.09s); the denoised image is shown in Fig. 2 (c). The corresponding cost value in (6) is $\Psi_{\text{orig}}(x) \approx 2534$. Then we apply the proposed approach by solving (20), with $\tau = 0.1$ in the algorithm, which converges to machine precision in about 400 iterations (computation time 73s). The obtained denoised image, shown in Fig. 2 (d), satisfies $|x_n^*| = 1$ and $r_{n,n'}^* = x_n^* x_{n'}^{**}$ for every (n, n') , so that it is the exact solution to the

original problem (6). The corresponding optimal cost value is $\Psi_{\text{conv}}^* = \Psi_{\text{orig}}^* \approx 2479$. By comparing the images in Fig. 2 (c) and (d), we can see that the image with the proposed method is a bit more regular, with less jagged level lines. We also show in Fig. 2 (e) the image obtained by replacing each pixel value by the weighted circular mean of its neighbors, with Gaussian weights, as described in Section II-E (computation time 0.003s); that is, we simply apply to y a convolution with a Gaussian filter (of standard deviation 3 pixels) and we rescale each value x_n to project it on the circle. The image is smooth and visually pleasant but its cost value is $\Psi_{\text{orig}}(x) \approx 2542$, similar to the one of the baseline method.

Our current implementation of the proposed algorithm is slow but it calls the eigendecomposition of every matrix to project it on the cone of positive semidefinite matrices. A careful implementation with a routine dedicated to this projection for 3×3 Hermitian matrices would reduce the computation time significantly.

It is not always the case that the proposed convex relaxation is tight and yields the solution to the original problem. For instance, if we keep the same experiment but with a noise standard deviation of 1 and $\lambda = 10$, the solution of (20) does not satisfy $|x_n^*| = 1$ for all n any more. We have $\Psi_{\text{approx}} = 6797 > \Psi_{\text{conv}}^* \approx 5953$. The baseline method yields an image x with a cost of $\Psi_{\text{orig}}(x) \approx 6749$. Both images are shown in Fig. 3. In particular, we can see that the proposed method has introduced an incorrect junction at the bottom right of the image in Fig. 3 (b). Elsewhere, it is more regular and probably closer to the exact solution of the problem (6) than with the baseline method. Thus, the proposed approach is best suited when the noise level is not too high.

C. Interpolation of a 1-D signal

We now consider interpolation at the intermediate indexes $n = 2, \dots, 9$ of the 1-D signal y defined at $n = 1$ and $n = 10$

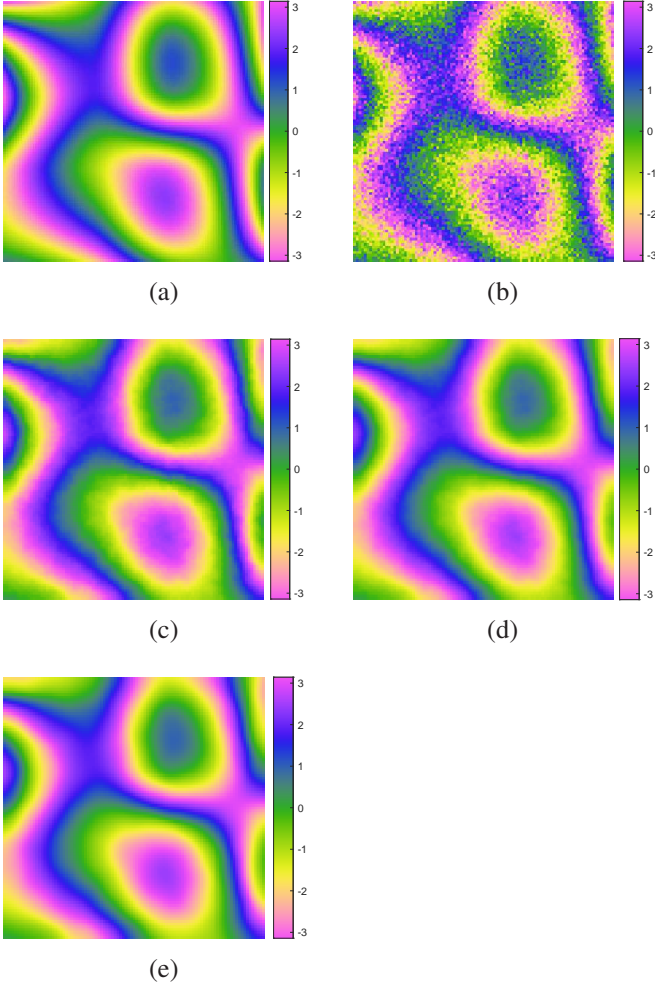


Fig. 2. Denoising of a circle-valued image: (a) the ground-truth image, (b) the noisy image, (c) the image denoised with the baseline method, (d) the image denoised with the proposed method, which turns out to be the exact solution to (4), (e) the image denoised by circular mean filtering with Gaussian weights. All images have their values in \mathbb{S} , whose argument in $(-\pi, \pi]$ is displayed, using the C2 cyclic colormap designed by Peter Kovesi [39].

by $y_1 = e^{-j}$ and $y_{10} = e^{2j}$. The problem we would like to solve is

$$\underset{x_n \in \mathbb{S} : n=1, \dots, 10}{\text{minimize}} \sum_{n=1}^9 \frac{1}{2} |x_{n+1} - x_n|^2 \quad \text{s.t.} \quad x_1 = e^{-j}, \quad x_{10} = e^{2j}. \quad (23)$$

It has a closed form solution: the points are uniformly distributed on \mathbb{S} , with $x_n = e^{j \frac{n-4}{3}}$; that is, the angles $\arg(x_n)$ linearly interpolate between $-\pi$ and 2π . The proposed convex relaxation is

$$\begin{aligned} & \underset{\substack{x_n \in \mathbb{C} : n=1, \dots, 10 \\ r_{n,n+1} \in \mathbb{C} : n=1, \dots, 9}}{\text{minimize}} \sum_{n=1}^9 (1 - \Re(r_{n,n+1})) \\ & \text{s.t.} \quad x_1 = e^{-j}, \quad x_{10} = e^{2j}, \quad \text{and} \\ & \begin{bmatrix} 1 & x_n^* & x_{n+1}^* \\ x_n & 1 & r_{n,n+1} \\ x_{n+1} & r_{n,n+1}^* & 1 \end{bmatrix} \succeq 0, \quad \forall n = 1, \dots, 9. \end{aligned} \quad (24)$$

We solve the problem using the Chambolle–Pock algorithm [37], [40], which is similar to the algorithm shown in Sec-

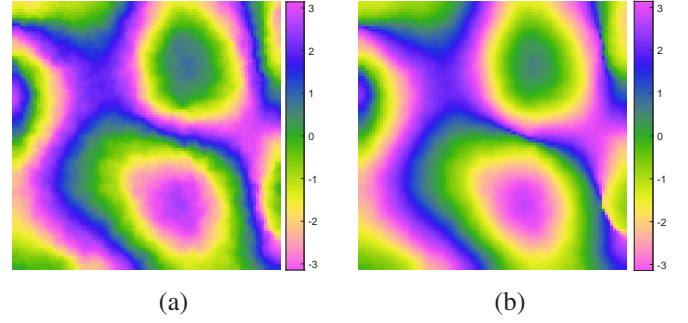


Fig. 3. Denoising of a circle-valued image, like in Fig. 2, but with the noise level and regularization parameter λ twice higher. (a) the image denoised with the baseline method, (b) the image denoised with the proposed method, which is only an approximate solution to (4).

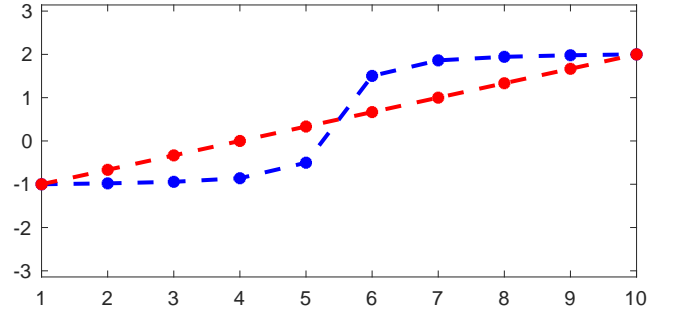


Fig. 4. Interpolation at $n = 2, \dots, 9$ between the fixed boundary values $y_1 = e^{-j}$ and $y_{10} = e^{2j}$. In blue, with the baseline method; in red, with the proposed method, which yields the expected solution; that is, a straight line.

tion IV, with additional enforcement of $x_1 = e^{-j}$, $x_{10} = e^{2j}$ at every iteration. Again, it turns out that the relaxation (24) is tight and we obtain the exact solution to (23). The interpolated signal is shown in Fig. 4, in red, and is uniform on \mathbb{S} , as predicted.

On the other hand, the baseline method consists in solving the convex problem

$$\underset{x_n \in \mathbb{C} : n=1, \dots, 10}{\text{minimize}} \sum_{n=1}^9 \frac{1}{2} |x_{n+1} - x_n|^2 \quad \text{s.t.} \quad x_1 = e^{-j}, \quad x_{10} = e^{2j}, \quad (25)$$

and then rescaling the obtained x_n as $x_n/|x_n|$ to project them on \mathbb{S} . We solved (25) using projected gradient descent, but the problem actually has a closed form solution, too: it is linear interpolation in \mathbb{C} , so that $x_n = \frac{n-1}{9} e^{2j} + \frac{10-n}{9} e^{-j}$. The interpolated signal is shown in Fig. 4, in blue. As we see, the angles of the x_n are not uniform in \mathbb{S} , so that the baseline method gives a bad approximate solution to the problem (23). This illustrates that the proposed convex relaxation is much tighter than the naive relaxation, which consists in reasoning in the disk \mathbb{D} instead of the circle \mathbb{S} .

VI. CONCLUSION

We proposed a new approach to smoothen or interpolate signals defined on the nonconvex complex circle, with a nonconvex formulation translating Bayesian estimation with von Mises priors, and a convex relaxation based on semidefinite

programming. We showed by experiments that the proposed relaxation is tight and yields the exact solution of the nonconvex problem in several cases. This opens the door to solutions of better quality for many applications involving circular data.

REFERENCES

- [1] P. A. Rosen, S. Hensley, I. R. Joughin, F. K. Li, S. N. Madsen, E. Rodriguez, and R. M. Goldstein, "Synthetic aperture radar interferometry," *Proc. IEEE*, vol. 88, no. 3, pp. 333–382, 2000.
- [2] S. Mosaddegh, L. Condat, and L. Brun, "Digital (or touch-less) fingerprint lifting using structured light," in *Proc. of Workshop on Forensics Applications of Computer Vision and Pattern Recognition (FACV)*, Santiago de Chile, Chile, Dec. 2015.
- [3] T. Lan, D. Erdogmus, S. J. Hayflick, and J. U. Szumowski, "Phase unwrapping and background correction in MRI," in *Proc. of IEEE Workshop on Machine Learning for Signal Processing (MLSP)*, Oct. 2008, pp. 239–243.
- [4] Y. Sowa, A. D. Rowe, M. C. Leake, T. Yakushi, M. Homma, A. Ishijima, and R. M. Berry, "Direct observation of steps in rotation of the bacterial flagellar motor," *Nature*, vol. 437, pp. 916–919, 2005.
- [5] J. Davis and R. Sampson, *Statistics and Data Analysis in Geology*. New York: Wiley, 2002.
- [6] J. Cremers and I. Klugkist, "One direction? A tutorial for circular data analysis using R with examples in cognitive psychology," *Front. Psychol.*, vol. 9, Oct. 2018, article 2040.
- [7] L. Ying, "Phase unwrapping," in *Wiley Encyclopedia of Biomedical Engineering*, M. Akay, Ed. Wiley, 2006.
- [8] J. M. Bioucas-Dias and G. Valadão, "Phase unwrapping via graph-cuts," *IEEE Trans. Image Process.*, vol. 16, no. 3, pp. 698–709, Mar. 2007.
- [9] L. Condat, D. Kitahara, and A. Hirabayashi, "A convex lifting approach to image phase unwrapping," in *Proc. of IEEE ICASSP*, Brighton, UK, 2019.
- [10] A. Chambolle, V. Caselles, D. Cremers, M. Novaga, and T. Pock, "An introduction to total variation for image analysis," in *Theoretical Foundations and Numerical Methods for Sparse Recovery*, vol. 9. De Gruyter, Radon Series Comp. Appl. Math., 2010, pp. 263–340.
- [11] L. Condat, "A direct algorithm for 1D total variation denoising," *IEEE Signal Process. Lett.*, vol. 20, no. 11, pp. 1054–1057, Nov. 2013.
- [12] —, "Discrete total variation: New definition and minimization," *SIAM J. Imaging Sciences*, vol. 10, no. 3, pp. 1258–1290, 2017.
- [13] D. Cremers and E. Strekalovskiy, "Total cyclic variation and generalizations," *J. Math. Imaging Vision*, vol. 47, pp. 258–277, 2013.
- [14] A. Weinmann, L. Demaret, and M. Storath, "Total variation regularization for manifold-valued data," *SIAM J. Imaging Sciences*, vol. 7, no. 4, pp. 2226–2257, 2014.
- [15] M. Storath, A. Weinmann, and M. Unser, "Exact algorithms for L^1 -TV regularization of real-valued and circle-valued signals," *SIAM J. Sci. Comput.*, vol. 38, no. 1, pp. A614–A630, 2016.
- [16] C. G. Khatri and K. V. Mardia, "The Von Mises–Fisher matrix distribution in orientation statistics," *Journal of the Royal Statistical Society*, vol. 39, no. 1, pp. 95–106, 1977.
- [17] R. Bergmann and D. Tenbrinck, "A graph framework for manifold-valued data," *SIAM J. Imaging Sciences*, vol. 11, no. 1, pp. 325–360, 2018.
- [18] A. Weinmann, L. Demaret, and M. Storath, "Mumford–Shah and potts regularization for manifold-valued data," *J. Math. Imaging. Vis.*, vol. 55, pp. 428–445, 2016.
- [19] M. Storath and A. Weinmann, "Variational regularization of inverse problems for manifold-valued data," *Information and Inference: A Journal of the IMA*, vol. 10, no. 1, pp. 195–230, 2021.
- [20] —, "Fast median filtering for phase or orientation data," *IEEE Trans. Pattern Anal. Mach. Intell.*, vol. 40, no. 3, pp. 639–652, 2018.
- [21] S. Di Zenzo, "A note on the gradient of a multi-image," *Computer Vision, Graphics, and Image Processing*, vol. 33, no. 1, pp. 116–125, Jan. 1986.
- [22] W. Förstner and E. Gülch, "A fast operator for detection and precise location of distinct points, corners and centres of circular features," in *Proc. of ISPRS Intercommission Conference on Fast Processing of Photogrammetric Data*, 1987, pp. 281–305.
- [23] M. Kass and A. Witkin, "Analyzing oriented patterns," *Computer Vision, Graphics, and Image Processing*, vol. 37, no. 3, pp. 362–385, Mar. 1987.
- [24] H. Knutsson, "Representing local structure using tensors," in *Proc. of 6th Scandinavian Conference on Image Analysis*, Jun. 1989, pp. 244–251.
- [25] J. Bigün, G. Granlund, and J. Wiklund, "Multidimensional orientation estimation with applications to texture analysis and optical flow," *IEEE Trans. Pattern Anal. Mach. Intell.*, vol. 13, pp. 775–790, 1991.
- [26] R. Meziat, "The method of moments in global optimization," *Journal of Mathematical Sciences*, vol. 116, no. 3, 2003.
- [27] C. Carathéodory, "Über den Variabilitätsbereich der Fourierschen Konstanten von positiven harmonischen Funktionen," *Rendiconti del Circolo Matematico di Palermo*, vol. 32, no. 1, pp. 193–217, 1911.
- [28] R. E. Curto and L. A. Fialkow, "Recursiveness, positivity, and truncated moment problems," *Houston J. Math.*, vol. 17, no. 4, pp. 603–635, 1991.
- [29] L. Condat, "Atomic norm minimization for decomposition into complex exponentials and optimal transport in Fourier domain," *Journal of Approximation Theory*, vol. 258, Oct. 2020.
- [30] C. Villani, *Topics in Optimal Transportation*, ser. Graduate studies in mathematics. American Mathematical Society, 2003.
- [31] J. Rabin, J. Delon, and Y. Gousseau, "Transportation distances on the circle," *Journal of Mathematical Imaging and Vision*, vol. 41, p. 147, Sep. 2011.
- [32] T. Werner, "A linear programming approach to max-sum problem: A review," *IEEE Trans. Pattern Anal. Mach. Intell.*, vol. 29, no. 7, pp. 1165–1179, 2007.
- [33] M. J. Wainwright and M. I. Jordan, "Graphical models, exponential families, and variational inference," *Found. Trends Mach. Learn.*, vol. 1, no. 1–2, pp. 1–305, 2008.
- [34] J. Kappes, B. Andres, F. Hamprecht, C. Schnörr, S. Nowozin, D. Batra, S. Kim, B. Kausler, T. Kröger, J. Lellmann, N. Komodakis, B. Savchynskyy, and C. Rother, "A comparative study of modern inference techniques for structured discrete energy minimization problems," *Int. J. Comput. Vis.*, vol. 115, no. 2, pp. 155–184, 2015.
- [35] J. P. R. Christensen and J. Vesterstrøm, "A note on extreme positive definite matrices," *Mathematische Annalen*, vol. 244, pp. 65–68, 1979.
- [36] R. T. Rockafellar, "Augmented Lagrangians and applications of the proximal point algorithm in convex programming," *Math. Oper. Res.*, vol. 1, pp. 97–116, 1976.
- [37] L. Condat, D. Kitahara, A. Contreras, and A. Hirabayashi, "Proximal splitting algorithms for convex optimization: A tour of recent advances, with new twists," *SIAM Review*, 2022, to appear.
- [38] H. H. Bauschke and P. L. Combettes, *Convex Analysis and Monotone Operator Theory in Hilbert Spaces*, 2nd ed. New York: Springer, 2017.
- [39] P. Kovési, "Good colour maps: How to design them," 2015, technical report arXiv:1509.03700, see also <https://colorcet.com>.
- [40] A. Chambolle and T. Pock, "A first-order primal-dual algorithm for convex problems with applications to imaging," *J. Math. Imaging Vision*, vol. 40, no. 1, pp. 120–145, May 2011.